https://doi.org/10.5194/egusphere-2023-215
Preprint. Discussion started: 17 April 2023

Measuring diameters and velocities of artificial raindrops with a neuromorphic dynamic vision sensor disdrometer

Jan Steiner[a,1], Kire Micev[a,1], Asude Aydin[b], Jörg Rieckermann[c], Tobi Delbruck[b,*]

[a]*Department of Mechanical and Process Engineering, ETH Zurich, Zurich, Switzerland*
[b]*Institute of Neuroinformatics (INI), University of Zurich and ETH Zurich (UZH-ETH), Zurich, Switzerland*
[c]*EAWAG, Swiss Federal Institute of Aquatic Science and Technology, Dübendorf, Switzerland*

Abstract

Hydrometers that can measure size and velocity distributions of precipitation are needed for research and corrections of rainfall estimates from weather radars and microwave links. Existing video disdrometers measure drop size distributions, but underestimate small raindrops and are impractical for widespread always-on IoT deployment. We propose an innovative method of measuring droplet size and velocity using a neuromorphic event camera. These dynamic vision sensors asynchronously output a sparse stream of pixel brightness changes. Droplets falling through the plane of focus create events generated by the motion of the droplet. Droplet size and speed are inferred from the stream of events. Using an improved hard disk arm actuator to reliably generate artificial raindrops, our experiments show small errors of 7% (maximum mean absolute percentage error) for droplet sizes from 0.3 to 2.5 mm and speeds from 1.3 m/s to 8.0 m/s. Each droplet requires the processing of only a few hundred to thousands of events, potentially enabling low-power always-on disdrometers that consume power proportional to the rainfall rate.

1. Introduction

There are increasing numbers of optical disdrometers that measure the diameter and speed of hydrometeors at ground level (X. Liu, Gao, and L. Liu 2013; Johannsen et al. 2020). Their Drop Size Distribution (**DSD**) measurements can be combined with weather radars or microwave links to predict a DSD over a larger area (Kruger and Krajewski 2002; Špačková et al. 2021). The State of the Art (**SoA**) scientific instrument is the 2-Dimensional Video Disdrometer (**2DVD**) first described by Kruger and Krajewski (2002)[2]. However, 2DVD and competing Particle Size Velocity (**PARSIVEL**) laser-sheet disdrometers have been reported to underestimate total rainfall volume and drift over time resulting in unpractical long-term deployment (Johannsen et al. 2020; Jaffrain and Berne 2011; Upton and Brawn 2008). Different types of disdrometers have been shown to produce measured DSDs that differ dramatically for small droplets (Johannsen et al. 2020; Cao et al. 2008). They are too expensive for ubiquitous deployment, and consume a lot of power on the order of 100 W making them impractical for solar-powered weather monitoring, where brownouts can occur in dark weather conditions (Špačková et al. 2021). Therefore, the ideal disdrometer would be precise and low-cost and would enable autonomous continuous DSD measurements by using less power when there are fewer droplets to measure.

In this paper, we propose using a novel droplet-driven sampling approach based on analyzing the brightness change events produce by a Dynamic Vision Sensor (**DVS**) event camera. Such an event camera does not capture stroboscopic images using a shutter as a conventional camera. Instead, each pixel reports asynchronous changes in brightness as they occur, and stays silent otherwise (Fig. 1A) (Lichtsteiner, Posch, and Delbruck 2008; Gallego et al. 2020). They have been successfully used in many high speed robotics and machine vision applications (Gallego et al. 2020), but not yet in environmental or atmospheric monitoring.

Our main contributions are:

1. We propose a novel optical disdrometer method that exploits the activity-driven output and high time resolution of DVS brightness change events to efficiently measure individual droplet size and

*Corresponding author
Email address: tobi@ini.uzh.ch (Tobi Delbruck)
[1]These authors contributed equally.
[2]See also www.distrometer.at

https://doi.org/10.5194/egusphere-2023-215
Preprint. Discussion started: 17 April 2023

speed using the shallow Depth of Field (**DoF**) of a fast lens to localize individual droplets in 3d space.

2. We generate high-quality ground-truth data for the droplets by modifying the Hard Disk Droplet Generator (**HDDG**) from Kosch and Ashgriz (2015) and report how to reproduce this HDDG.
3. We report the first measurements of droplet size and speed with our proposed Dynamic Vision Sensor Disdrometer (**DVSD**) and show that the DSD satisfactorily aligns with the ground truth data with at most a mean absolute percentage error of 7%.

2. Materials and Methods

2.1. DVSD Setup

Fig. 1 illustrates our proposed DVSD method, which is detailed in our Supplementary Material (**SM**) Secs. S.2 and S.3. The DVS camera (Fig. 1A, SM Sec. S.1) asynchronously reports brightness change events as the droplets pass through a thin DoF at the Plane of Focus Rectangle (**PoFR**) from a lens that looks down on the rainfall from a steep angle (Fig. 1B). Each droplet produces a few hundred to a few thousand DVS brightness change events. By a simple analysis of this cluster of events, the DVSD can measure both the size and the speed of the droplet. We developed a modified HDDG to generate small droplets and used an Intravenous Dripper Droplet Generator (**IVDG**) for large droplets. Fig. 1C shows an illuminated falling water droplet recorded with the DVS camera. Our method consists of two key principles. First, we aim the camera downward at a steep angle, with an angle α from the vertical (Fig. 1B: left). Second, the diameters of the droplets crossing the shallow DoF at the Plane of Focus (**PoF**) are measured unambiguously, *i.e.*, since the PoF is located at a fixed working distance from the lens, we can infer the 3d position of the droplet, and hence disambiguate the absolute size from the image size. Droplets passing through the camera's PoF come into focus, showing a high contrast, whereas droplets outside the PoF appear blurry. Therefore, droplets that are out of focus cover a larger area of the recording than when they are in focus (see Fig. 1C: black circles). Accumulating the events belonging to one droplet that crosses the PoFR (marked by * in figure) produces an hourglass shape (Fig. 1C: accumulated events) where the ideal moment for a droplet diameter measurement (Sec. S.4.10) is at the waist of this hourglass. The hourglass should be as concave as possible to facilitate the detection of the waist. Using a fast lens with a small aperture ratio f number produces a shallow DoF, increasing the amount of blur of the droplets that are out of focus. Fig. 1B also illustrates how a droplet that crosses the field of view (**FoV**) but past the PoFR (marked by # in figure) creates an accumulated image that starts out blurry and becomes increasingly blurry until it leaves the FoV; similarly (but not illustrated), a droplet that crosses the FoV in front of PoFR creates an accumulated event image that starts out blurry and becomes increasingly sharper until it leaves the FoV. Only droplets that cross the PoFR create hourglasses.

2.2. Modification of the HDDG

Fig. 1D and SM Sec. S.2 and Figs. S2 and S3 illustrate our HDDG. It is based on previous work by Kosch and Ashgriz (2015), who utilized a computer hard disk arm as an actuator. They used a high-frequency buzz to create ripples in a steady stream of water emitted by a stiff glass needle, which would break up into small droplets. Our HDDG uses a flexible plastic needle, which, if properly combined with a steady stream of water, creates a single droplet at each end of an oscillation, resulting in two droplet streams, one of which we measured. We used a discarded hard disk drive that we disassembled to expose the platter head actuator arm. The arm is coupled to the needle by threading the needle through adhesive tape applied over the hole in the arm allowing the needle to protrude. The arm is actuated with a home audio power amplifier driven by sinusoidal waveforms generated by an audio wave generating program where we used coil driver amplitudes from 5 Vpp–20 Vpp and frequencies from 60 Hz–220 Hz.

3. Results

We conducted two series of experiments, one with the HDDG and one with the IVDG (SM S.2). We used different lenses to make it easier to capture droplets crossing the PoF. The droplets created by the HDDG ranged from 0.3 mm to 0.6 mm (10 to 20 pixel diameter on the image), while the droplets created by the IVDG were 2.5 mm (17-18 pixel diameter). In both experiments, the height of the fall was sufficient for the droplets to reach within 97% of the terminal speed (SM S.5). Fig. 2 compares the measurement results performed with the DVS (see S.4.10) to ground truth (**GT**) (see SM S.4.11

https://doi.org/10.5194/egusphere-2023-215
Preprint. Discussion started: 17 April 2023

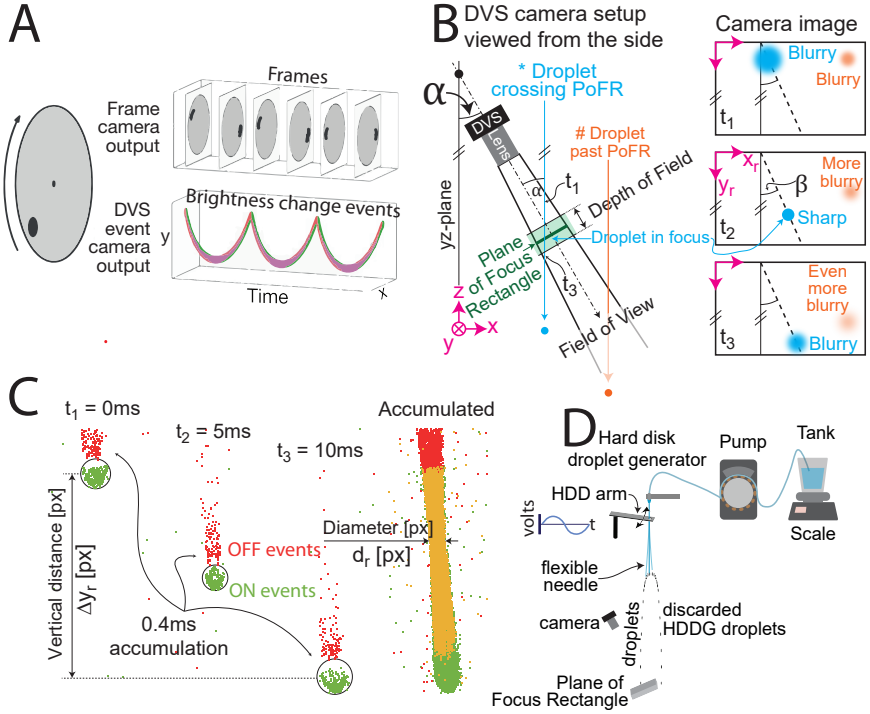

Figure 1: Summary of Dynamic Vision Sensor Disdrometer (DVSD) methods. A: Comparison between a conventional frame camera and a DVS capturing a rotating disk with a black dot. The frame camera outputs frames with finite exposure duration at discrete time intervals, whereas the event camera continuously outputs brightness change events, which results in a helix of discrete events in the space time plot (green: increase in brightness, red: decrease in brightness) (Lichtsteiner, Posch, and Delbruck 2008; Gallego et al. 2020) (SM S.1). **B**: Side view of the DVS camera setup in experiments and three illustrations of DVS recordings. The cyan droplet enters and exits the FoV, which is tilted at a small angle α from the vertical yz-plane; we used 22 for HDDG and 29 for IVDG experiments. The corresponding recording is illustrated on the right side at three different times: the cyan droplet entering the FoV, droplet crossing the PoF, and droplet exiting the FoV. β is the angle of the droplet from the vertical y_r-axis seen on the recording, caused by droplet velocity component in the yz-plane (out of the page) resulting from the HDDG. The orange droplet never crosses the PoF and only grows increasingly blurry. (SM S.3,S.4) **C**: Sample DVS recording of a droplet crossing the PoF, which is demonstrated in three frames with 5 ms time differences between each frame. Each of the three DVS frames in this sample is an accumulation of 0.4 ms of events. Green points correspond to ON events, red points show OFF, and yellow points show overlapping of ON and OFF events. The rightmost frame shows all accumulated events over 10 ms. Each droplet creates several hundred to several thousand events, depending on its size. We estimate the falling speed v_r by measuring the focal plane speed of the droplet. The diameter d_r of the droplet is measured at the waist of the hourglass when the droplet is in focus, as illustrated on the right. Eqs. (S6) and (S7) provide the droplet diameter and speed. (SM S.4.10) **D**: HDDG modified from Kosch and Ashgriz (2015). The droplet generator uses a hard disk actuator to oscillate a flexible needle with a constant flow rate of water fed into the needle from a pump. The water tank is placed on top of a scale to calculate the flow rate. Within a 4× range of oscillation frequencies, a droplet is released at each end of the oscillation by large acceleration forces acting on the flexible needle. The diameter of droplets released from the needle is adjusted by the oscillation frequency of the needle. We generated the large 2.5 mm droplets falling 10 m through a circular staircase well with an intravenous (**IV**) dripper. (SM S.2 S.3)

and S.5). The HDDG droplets (green data points) are magnified for better visibility, and the IVDG droplets (purple data points) have a purple histogram beside them, indicating the number of measurement results that overlap.

https://doi.org/10.5194/egusphere-2023-215
Preprint. Discussion started: 17 April 2023

The results show excellent linearity over the entire measurement range for both size and speed; the dashed line in each plot has a slope of one and passes through the origin; it lies close to both small and large droplet measurements. Size measurements slightly overestimate small droplet diameters, and speed measurements slightly underestimate large droplet speeds. The quantization of the data arises from the quantized droplet size generation and the pixel discretization. Horizontal quantization is caused by the quantized HDDG droplet creation frequencies, which control the diameters of the droplets. Vertical quantization is caused by the low pixel count of the diameter of the droplets in the DVS recording. The speed measurements do not have any significant vertical quantization effects, due to large pixel displacements (≈ 100 pixels) and the fine DVS event timestamp resolution of 1 µs.

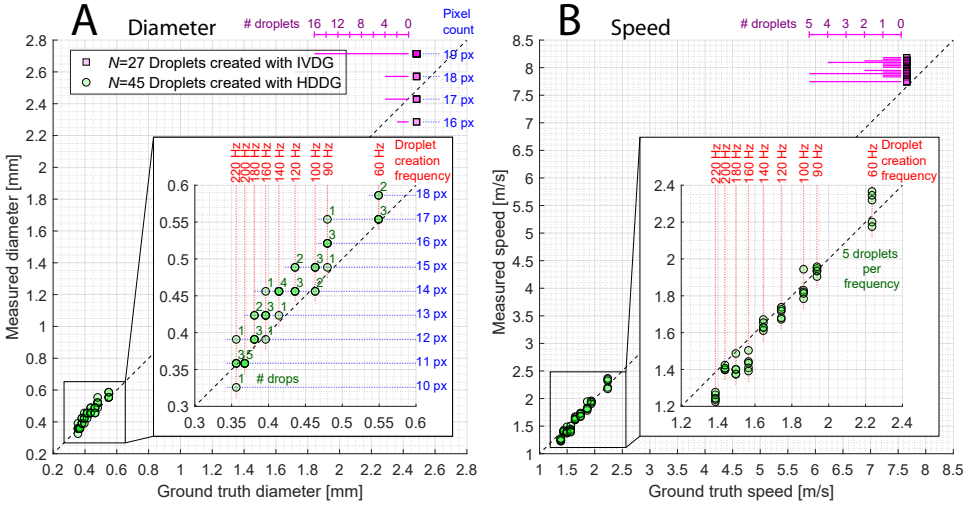

Figure 2: Main results. DVSD measurement results of droplets compared to GT values, where **A** shows the diameter and **B** shows the velocity. The dashed black line represents a 45°-line passing through the origin. Both drop creation methods are included in the plots. The zoomed plots show droplets created with the HDDG for improved visibility. Numbers adjacent to the points on the left zoomed plot indicate overlaps whereas the zoomed plot on the right has 5 droplets per frequency. The IVDG droplets are shown in purple with a histogram for number of overlapping points. Quantization effects caused by the pixel count or frequency are illustrated as a grid pattern in the plots where the effect is significant. (See SM S.4 for details.)

We used Mean Absolute Percentage Error (**MAPE**) to further quantify the discrepancy between the ground truth values and the DVS measurements (SM S.4.2). Table 1 lists the diameter and velocity MAPE for both experiments. In all cases, MAPE remains below 7%.

Mean absolute percentage error

Experiment	Diameter	Velocity
HDDG	6%	4%
IVDG	7%	4%

Table 1: MAPE of the DVS measurements compared to GT values, for the diameter and velocity measurements from both experiments.

Table 2 lists the estimated combined uncertainties of the measured diameter and velocity using the method explained in SM S.4.2. In some cases, a range of uncertainties is given, which means the uncertainty depends on the size of the droplet. The combined uncertainty percentage is largest for the DVS measurement of the smallest droplets created with the HDDG, which had a diameter of 0.35 mm ± 0.03 mm (±10%). This large uncertainty is caused by the low pixel diameter count (≈ 10 pixels).

The uncertainty (*i.e.*, precision) of DVSD diameter and velocity measurements are mainly limited by the spatial resolution of the 346 × 260-pixel DVS (see Table 2: bottom). The GT diameter uncertainty (see Table 2: top) was mostly caused by the measurement uncertainty of the scale and noise in the droplet

https://doi.org/10.5194/egusphere-2023-215
Preprint. Discussion started: 17 April 2023

generation by the HDDG and IVDG. The GT velocity uncertainty arises from neglecting air turbulence, droplet deformation, and inaccurate sphere model values, i.e. GT droplet diameter estimates from mass flow. The GT droplet diameter and velocity are calculated from their mass and from the simulation, respectively (see S.2 and S.5). Therefore, if the diameter is uncertain, it increases velocity uncertainty.

Combined uncertainty

Method	Experiment	Diameter		Velocity	
		±[%]	±[mm]	±[%]	±[m/s]
GT	HDDG	3	0.01–0.02	4–7	0.1
	IVDG	2	0.05	4	0.3
DVS	HDDG	6–10	0.03	7	0.1–0.2
	IVDG	6–7	0.15	6	0.5

Table 2: Percentage and absolute combined uncertainty of the DVS measurements and GT values for diameter and velocity.

4. Discussion

4.1. Experimental results

Although the large droplets were generated and measured differently than the small droplets, the two data sets are very consistent (see Fig. 2: green and purple data sets). The offset of the data points from the 45°-line (see Fig. 2) is correctable since it arises from slightly inaccurate α and M estimates. Therefore, we believe that the DVSD can achieve accurate droplet measurements.

We used a shorter lens for the larger IVDG droplets only to allow us to capture the large droplets more easily, since they scattered much more from random wind currents in the staircase than the small droplets from the HDDG. It is possible to obtain better precision of large droplets by using the same lens, but with the trade-off of longer experiment time since fewer will pass through the PoFR.

Future studies should compare the DVSD directly to SoA disdrometers that measure individual droplet diameters and velocities. Improving our HDDG should be investigated since our HDDG was somewhat unstable, which required patience to capture sufficient good droplets to measure (SM S.2.3). Using Near Infrared (**NIR**) illumination should also be tried, since most insects would be blind to it and hence not be attracted to the DVSD, and DVS silicon photodiodes work well with NIR illumination.

4.2. Limitations of experiments

Our experiments were carried out in a controlled environment using two droplet generators, i.e. HDDG and IVDG. However, unlike real rainfall conditions, there were no strong winds. Moreover, the drop jets were localized and did not occlude each other. We do not believe that occlusion would be a problem due to the optical arrangement, but the droplet tracks could merge or overlap and the droplets in front or behind the PoF could disturb the measurements. Therefore, it is difficult to predict how well a DVSD would perform under windy conditions or with heavy rainfall.

Our *hourglass* DVSD method (SM S.4.10) works best when the droplets pass all the way through the FoV (see Fig. 1B: left, and Fig. S5: bottom left corner). In an extreme case, the wind could make a droplet trajectory parallel to the Line of Sight (**LoS**) of the camera. If this is the case, no hourglass would be visible on the DVS recording after an accumulation of events; from the point of view of the DVS, the droplets would appear to shrink and grow while slowly drifting in a random direction. In principle, it should be possible to infer the 3d trajectory of the droplet by developing an algorithm that continuously estimates the diameter and velocity of the droplets. We would base such algorithm on cluster trackers commonly used for other DVS applications (Delbruck and Lang 2013; Gallego et al. 2020). These trackers would initiate clusters at the top of the FoV, and then use brightness change events to track the droplets, while measuring the droplet velocity and diameter. A simple set of plausibility checks on the cluster path and a fit to the hourglass diameter samples could provide the image plane droplet measurements along with their uncertainties.

The size of the sampling area plays an important role in how quickly a DSD can be obtained. The sampling area of the DVSD decreases slightly with increasing drop size, because the droplets must be fully inside and pass through the FoV. Therefore, a correction will be needed to estimate the DSD to account for the smaller fraction of larger droplets that are measured.

If our DVS were required to have the same sampling area as the OTT Parsivel^2 (see Table 3), a reduction in focal length would be necessary, but would increase the current 0.35 mm drop size uncertainty

https://doi.org/10.5194/egusphere-2023-215
Preprint. Discussion started: 17 April 2023

Table 3: Comparison of disdrometer specifications. Data may not be accurate for latest models.

Specification	Device		
	DVSD[1]	2DVD[2]	PARSIVEL[3]
Technology	1 dynamic vision sensor	2 line-scan cameras	Laser-sheet
Sensor resolution	346 × 260	512 px	1 photodetector
Pixel pitch	18.5μm	NA	none
Power	3 W camera + 40 W LED	500 W	100 W
Data rate	variable (0-1MB/s)	80 MB/s	2.4 MB/s
Optics	300mm (HDDG) 75mm (IVDG)	NA	NA
Sampling area	0.88 cm^2 (HDDG) 400mm cm^2 (IVDG)	100 cm^2	54 cm^2
Diameter range	0.3–0.6 mm (HDDG) 2.5 mm (IVDG)	0.1–9.9 mm	0.2–8.0 mm
Speed range	1–8 m/s	all	0.2–20.0 m/s
Diameter precision	±0.03 mm (HDDG)	±0.19 mm	±2 mm for small
Speed precision	±6% (HDDG)	±4%	±5%

[1] DAVIS346 from www.inivation.com, based on Taverni et al. (2018) FSI sensor chip.
[2] Kruger and Krajewski 2002
[3] *OTT Parsivel^2 - Laser Weather Sensor* 2016

from 10% (see Table 2) to 75%. However, these limitations are a result of the low spatial resolution of our prototype camera and megapixel DVS are already available (Suh et al. 2020; Finateu et al. 2020). With a megapixel DVS, the 0.35 mm droplet size uncertainty would be about 20% while matching the sampling area of the OTT Parsivel^2 by adjusting the focal length to the appropriate value.

4.3. Comparing DVSD to other optical disdrometers

Table 3 compares the specifications of our current DVS prototype to the OTT Parsivel^2 and 2DVD. Other optical disdrometers measure the size of the droplets by the size of the 1D occlusion (2DVD) or the decrease in the intensity of light (PARSIVEL). The DVSD takes advantage of the ability of DVS to finely measure the velocity of the droplet across the plane of focus and uses the PoF to locate the droplet in space for unambiguous size measurement.

The measurement uncertainty of the DVSD is in a range similar to that of other optical disdrometers; field experiments with co-located instruments resulted in about 5%–11% error in small drops (D0 = 1–2 mm) and the error varies from approximately 8% to 4.5% at D0 = 1.5 mm from 1 min to 10 min sampling time (Jaffrain and Berne 2012; Chang et al. 2020).

Johannsen et al. (2020) reported difficulty with long-term measurements using PARSIVEL and 2DVD because of drift and insect and spider debris accumulating in optical housings. The simpler free-space optical arrangement of the DVSD could be advantageous in avoiding these problems. Speed is measured by the time of passage between nearby light sheets (2DVD) or by the time that a single light sheet is occluded (PARSIVEL) (Johannsen et al. 2020). Both techniques require high sample rates because droplets that fall at a terminal speed pass through any given point in a few hundred microseconds. *E.g.*, a 1 mm droplet falling at its terminal speed of 4 m/s (SM S.5) passes by in only 250 μs. The 1 μs time resolution of DVS allows very accurate measurements of droplet speed in the image plane, but at a low camera data rate of a few hundred to thousand brightness change events per droplet, which could easily be processed by an embedded microcontroller.

5. Conclusions

Our paper proposes an innovative way to measure droplets using an activity-driven DVS event camera that observes the droplets falling through a shallow DoF. Our results demonstrate the feasibility of this DVSD method for droplets ranging from 0.3 mm to 2.5 mm, covering most of the real rainfall range. Droplet size and velocity measurements from the DVSD have a maximum of 7% MAPE compared to the ground truth from the drop generator. The droplet size uncertainties of the DVSD measurements and GT values are 10% and 3% respectively, whereas the droplet velocity uncertainties are both 7%. The uncertainty of our prototype is encouraging because we expect substantial potential for improvement through more advanced hardware and processing methods. Most of all, our results are virtually unbiased, especially for small drops, which are difficult to observe for existing optical disdrometers.

With our strongest magnifying lens, our DVSD prototype—under laboratory conditions—surpasses SoA disdrometers in terms of precision even though the sampling area is much smaller, as Table 3

https://doi.org/10.5194/egusphere-2023-215
Preprint. Discussion started: 17 April 2023

shows. For future work, our aim is to increase the sensor resolution and capture real rainfall data with comparisons to SoA disdrometers.

Today, the installation of multiple DVSDs would be expensive due to the prototype costs of the DVS cameras. However, mass production for DVS applications in consumer electronics will rapidly decrease production cost and improve the resolution and quality of DVS cameras. A DVSD based on a low-power, inexpensive embedded Linux microcomputer could be developed that can autonomously estimate droplet diameters and velocities in real time while surviving harsh weather conditions in remote areas disconnected from the power grid. The rain-driven computation and simple optical and lighting requirements of a DVSD would be a great advantage compared to alternative optical disdrometers that sample at a constant high rate and require more complex optical and lighting arrangements.

Data availability and Supplementary Material

Our Supplementary Material details our materials and methods and our raw data and videos are available online[3].

Author contributions

J. Steiner and K. Micev performed most of the experimental work and data analysis. A. Aydin performed initial experiments to establish the concept. T. Delbruck and J. Rickermann conceived and supervised the project. All authors participated in the writing of the paper.

Competing interests

The authors declare that they have no conflict of interest.

Acknowledgments

We thank J.P. Carbajal (Ostschweizer Fachhochschule) for catalyzing this collaboration, G. Taverni (formerly UZH-ETH) for help with initial feasibility studies, S. Kosch (aldusleaf.org), N. Ashgriz (U. Toronto), and R. Loidl (UZH-ETH) for their advice on HDDG.

References

Cao, Q. et al. (2008). "Analysis of video disdrometer and polarimetric radar data to characterize rain microphysics in Oklahoma". In: *J. Appl. Meteor. Climate* 47.8, pp. 2238–2255. DOI: 10.1175/2008JAMC1732.1.

Chang, Wei-Yu et al. (Apr. 2020). "Uncertainty in Measured Raindrop Size Distributions from Four Types of Collocated Instruments". In: *Remote Sensing* 12.7, p. 1167. ISSN: 2072-4292, 2072-4292. DOI: 10.3390/rs12071167.

Delbruck, Tobi and Manuel Lang (2013). "Robotic goalie with 3 ms reaction time at 4% CPU load using event-based dynamic vision sensor". In: *Frontiers in neuroscience* 7, p. 223. DOI: 10.3389/fnins.2013.00223.

Finateu, T et al. (Feb. 2020). "5.10 A 1280×720 Back-Illuminated Stacked Temporal Contrast Event-Based Vision Sensor with 4.86µm Pixels, 1.066GEPS Readout, Programmable Event-Rate Controller and Compressive Data-Formatting Pipeline". In: *2020 IEEE International Solid- State Circuits Conference - (ISSCC)*, pp. 112–114. DOI: 10.1109/ISSCC19947.2020.9063149.

Gallego, Guillermo et al. (July 2020). "Event-based Vision: A Survey". In: *IEEE Trans. Pattern Anal. Mach. Intell.* PP, pp. 1–1. ISSN: 0162-8828. DOI: 10.1109/TPAMI.2020.3008413.

Jaffrain, Joël and Alexis Berne (2011). "Experimental quantification of the sampling uncertainty associated with measurements from PARSIVEL disdrometers". In: *Journal of Hydrometeorology*. Publisher: American Meteorological Society. ISSN: 1525-755X. DOI: 10.1175/2010JHM1244.1.

— (Apr. 2012). "Influence of the Subgrid Variability of the Raindrop Size Distribution on Radar Rainfall Estimators". In: *J. Appl. Meteorol. Climatol.* 51.4, pp. 780–785. ISSN: 1558-8424, 1558-8432. DOI: 10.1175/JAMC-D-11-0185.1.

Johannsen, Lisbeth Lolk et al. (Mar. 2020). "Comparison of three types of laser optical disdrometers under natural rainfall conditions". In: *Hydrological Sciences Journal* 65.4, pp. 524–535. ISSN: 0262-6667. DOI: 10.1080/02626667.2019.1709641. (Visited on 01/05/2022).

[3]Raindrop measurement with event camera

https://doi.org/10.5194/egusphere-2023-215
Preprint. Discussion started: 17 April 2023

Kosch, Sebastian and Nasser Ashgriz (Apr. 2015). "Note: A simple vibrating orifice monodisperse droplet generator using a hard drive actuator arm". In: *Rev. Sci. Instrum.* 86.4, p. 046101. ISSN: 0034-6748, 1089-7623. DOI: 10.1063/1.4916703.

Kruger, A. and W. F. Krajewski (2002). "Two-dimensional video disdrometer: a description". In: *J. Atmos. Oceanic Technol.* 19.5, pp. 602–617. DOI: 10.1175/1520-0426(2002)019<0602:TDVDAD>2.0.CO;2.

Lichtsteiner, Patrick, Christoph Posch, and Tobi Delbruck (Feb. 2008). "A 128×128 120 dB 15 μs latency asynchronous temporal contrast vision sensor". In: *IEEE J. Solid-State Circuits* 43.2, pp. 566–576. ISSN: 0018-9200, 1558-173X. DOI: 10.1109/jssc.2007.914337.

Liu, XC, TC Gao, and L Liu (2013). "A comparison of rainfall measurements from multiple instruments". In: *Atmospheric Measurement Techniques* 6.7, pp. 1585–1595. DOI: 10.5194/amt-6-1585-2013.

OTT Parsivel^2 - Laser Weather Sensor (2016). https://www.ott.com/products/meteorological-sensors-26/ott-parsivel2-laser-weather-sensor-2392/. Accessed: 2022-3-27. URL: https://www.ott.com/products/meteorological-sensors-26/ott-parsivel2-laser-weather-sensor-2392/.

Špačková, A. et al. (2021). "A year of attenuation data from a commercial dual-polarized duplex microwave link with concurrent disdrometer, rain gauge, and weather observations". In: *Earth System Science Data* 13.8, pp. 4219–4240. DOI: 10.5194/essd-13-4219-2021.

Suh, Yunjae et al. (2020). "A 1280× 960 Dynamic Vision Sensor with a 4.95-μm Pixel Pitch and Motion Artifact Minimization". In: *2020 IEEE International Symposium on Circuits and Systems (ISCAS)*. IEEE, pp. 1–5. DOI: 10.1109/ISCAS45731.2020.9180436.

Taverni, G et al. (May 2018). "Front and Back Illuminated Dynamic and Active Pixel Vision Sensors Comparison". In: *IEEE Trans. Circuits Syst. Express Briefs* 65.5, pp. 677–681. ISSN: 1558-3791. DOI: 10.1109/TCSII.2018.2824899.

Upton, Graham and Dan Brawn (2008). "An investigation of factors affecting the accuracy of Thies disdrometers". In: *WMO Technical Conference on Instruments and Methods of Observation (TECO-2008), St. Petersburg, Russian Federation*. researchgate.net, pp. 27–29. URL: https://www.researchgate.net/profile/Graham-Upton/publication/237690271_An_investigation_of_factors_affecting_the_accuracy_of_Thies_disdrometers/links/004635205f951d54ee000000/An-investigation-of-factors-affecting-the-accuracy-of-Thies-disdrometers.pdf.